COMMISSIONS G1 AND G4 OF THE IAU
INFORMATION BULLETIN ON VARIABLE STARS
Volume 63 Number 6266 DOI: 10.22444/IBVS.6266

Konkoly Observatory
Budapest
8 May 2019

HU ISSN 0374 – 0676

RZ COMAE – A W-TYPE OVERCONTACT ECLIPSING BINARY

NELSON, R.H.[1,2,3]; ALTON, K.B.[3,4]

[1] Mountain Ash Observatory, 1393 Garvin Street, Prince George, BC, Canada, V2M 3Z1 email: bob.nelson@shaw.ca

[2] Guest investigator, Dominion Astrophysical Observatory, Herzberg Institute of Astrophysics, National Research Council of Canada

[3] Desert Bloom Observatory, Benson AZ, 31°56′.454 N, 110°15′.450 W

[4] UnderOak Observatory, 70 Summit Ave, Cedar Knolls, NJ, USA, email: kbalton@optonline.net

Abstract

RZ Com (GSC 1990-2841) is a short period (P = 0.3385 d) W UMa–type binary system, type–W, which has had, over the years, two spectroscopic and numerous light curve studies. The various mass determinations show a large scatter. Here we present the results of new light curve and radial velocity observations, and a fresh analysis by the Wilson-Devinney 2003 code. We have been able to obtain a unified model for photometric five datasets, each used one or more filters. The main model parameters such as mass ratio, temperature, potential, and inclination were in close agreement, as were derived quantities such as mass, stellar radius, etc. Only the spot parameters differed, as one might expect. Further, we determined a distance estimate, r = 204 ± 5 pc, in good agreement with the *Gaia* value of r = 203.1 ± 3.7 pc. We also presented four new eclipse timings, performed a renewed period analysis attaining a LiTE fit. With that we determined a rate of intrinsic period change $dP/dt = 3.86(2) \times 10^{-8}$ days/year, and–assuming conservative processes–a rate of mass exchange $dm_1/dt = -4.1(3) \times 10^{-8}\, M_\odot$/year which means that the less massive star is losing mass to its companion.

The identity of the discoverer of the variability of RZ Com (AN 5.1929; TYC 1990-2841-1) is not clear. However, we do know that S. Gaposchkin (1932, 1938) obtained early photometric light curves and times of minima, and deduced an inclination of 81°. Likely it was he who first identified the system as a W Ursae Majoris type.

Thereafter, Struve & Gratton (1948) performed spectrographic observations at the McDonald Observatory using the 2.08-m reflector, the f/2 Schmidt camera, the Cassegrain spectrograph with its glass prisms, and 103a-O film. As the reciprocal dispersion was 76 Å/mm, there was considerable scatter in their radial velocity (RV) plots (rms deviation from curves of best fit 36 km/s). However, they did deduce a spectral type of 'approximately' K0, a system velocity of -12 km/s, amplitudes K_1 and K_2 of 270 and 130 km/s respectively, and therefore a mass ratio of $q = m_2/m_1 = 2.1$. Further, they also observed that the more massive component was eclipsed at secondary minimum. (This type of system, later described as W-Type by Binnendijk (1970), features the hotter, less massive star eclipsed at primary minimum. That event, the deeper eclipse, is then an occultation, resulting in a short interval of constant light. We will follow the convention of designating that star as m_1, hence mass ratios of $q = m_2/m_1 > 1$ will ensue.)

Kopal (1955) in his classification of some 63 close binary systems listed RZ Com with solar masses of 0.8 and 1.6, spectral types of G9 and K0, and $\log T$ (temperature) values

of 3.72 and 3.71 respectively [corresponding to $T_1 = 5250$ K and $T_2 = 5230$ K]. The next photometric observations were by Broglia (1960) using a yellow ($\lambda = 5300$ Å) filter. Although the paper is unavailable, Binnendijk (1964) described the normal (binned) results and kindly reproduced the data. Thus, in 1958 Broglia obtained two sets of these light curves within an interval of about four months, and noted changes to the light curve during that interval. The primary minima, with short periods of constant light (during the total eclipses), were the same, but the second light curve was about 0.02 magnitudes brighter everywhere else. Binnendijk (1964) analyzed the light curves of Broglia using the rectification method, and determined (amongst other things) an inclination of 81.1°. He then combined the RV elements from Struve & Gratton (1948) to obtain masses of $m_1 = 0.77\,M_\odot$ and $m_2 = 1.59\,M_\odot$. Broglia had assumed that the differences in the light curves could be explained by a change in the outer surface of the smaller component during secondary eclipse. However, because of the asymmetry in the light curves, Binnendijk suggested that the effect could be better explained by an asymmetrically positioned subluminous region (viz., a dark spot) on the facing (back) side of the larger star.

Pointing out that the Russell-Merrill (1952) rectification method breaks down for contact binaries, (Wilson & Devinney, 1973) discussed progress in physical models to that date (see references therein). Promoting the advantages of their newly published physical light curve analysis package Wilson & Devinney (1971), they then re-analyzed the photometric data of Broglia (1960) along with the radial velocity data of Struve & Gratton (1948). However, in an apparent effort to illustrate systems that could be analyzed by mode 1 (overcontact, $T_1 = T_2$), they made some unorthodox assumptions. Admitting that using radiative atmospheres was unusual for G9+K0 systems, they went ahead anyway and allowed the gravity exponent g to vary, obtaining the very different values of $g = 1.13$ and 1.51 for data taken for the same binary system separated by only two or three months. An anonymous referee pointed out that the 1973 W–D code did not include the capability of adding spots; hence that might explain the "strange gravity darkening exponents".

They also concluded that the system was in marginal contact, with the first data set indicating slightly overcontact and the second, undercontact. [Using their values for the mass ratio and potential, we found the fillout parameters to be 0.0418 and −0.0589, respectively.] It does not seem possible to us on physical grounds that the system could change so significantly on such a short time span. In their paper there is no discussion of the possibility of a star spot or of third light. In view of their unphysical assumptions, one might be tempted to reject their results entirely; however the closeness of their curve fits causes one to pause. At the very least, the situation raises unsettling questions about uniqueness of WD solutions.

The next spectroscopic observations were by McLean & Hilditch (1983) at the Dominion Astrophysical Observatory (DAO) at Victoria, B.C., Canada using the 1.83-m Plaskett telescope, the Cassegrain spectrograph, and IIa-O plates. Reciprocal dispersion was 30 Å/mm. Although there was moderate scatter in their data [rms deviation from curves of best fit ~ 25 km/s], they did deduce a system velocity of −1.8(5) km/s, and amplitudes K_1 and K_2 of 248.0(9) and 107.0(6) km/s respectively.

Thereafter photometric observations were taken by Rovithis & Rovithis-Livaniou (1984) at the Kryonerion Astrophysical Station in Greece, using the 1.2 m Cassegrain reflector with a two-beam multi-mode photometer. Their published data, in B and V light, display an unusual shape and although nine new times of minima were reported, they made no attempt to model the data. Numerous attempts by the lead author at modelling their light curves (which more represent those of a detached system) all failed. Therefore the validity of their data must remain questionable.

Table 1: Various determinations of the RZ Com spectral type.

Reference	Sp. Type
Struve & Gratton (1948)	K0
Wood et al. (1980)	F7+K0
Batten et al. (1989)	G2Vn
Perryman et al. (1997) - Hipparcos Cat.	G0Vn

Rovithis-Livaniou et al. (2002) also published a paper attempting to analyze the period variations; however the listed data—while numerous—did not allow for any meaningful conclusions about the period behaviour due to the limited time interval spanned by the data. In addition, they did point to the lack of agreement as to the spectral type, referencing four disparate classifications. These are given in Table 1.

Xiang & Zhou (2004) obtained a B band light curve at the Yunan Observatory in China using the 1.00-m reflector telescope and a CCD camera. They extracted five new times of minima from their published data and proceeded to perform a photometric analysis using the 1992 version of the Wilson-Devinney code. Using the 'q-search' method they obtained two solution sets with mass ratio values of 0.8 and 2.2 and "[could not] say which of the two results is accurate". This is in spite of the fact that there were two radial velocity datasets available Struve & Gratton (1948); McLean & Hilditch, (1983) which would have resolved the issue. Unfortunately, there also seemed to be some confusion between the different naming conventions (for m_1 and m_2) typically used by spectroscopists and photometrists.

Lastly, Qian (2001) and Qian & He (2005) presented period analyses. The latter paper presented four new times of minima and a light time effect (LiTE) analysis of the—by now—extensive data set. The analysis was updated in a review paper by Nelson et al. (2016), who obtained similar results. Both LiTE fitting results, along with those of this paper, are presented in Table 14.

Because more modern techniques promised to improve the radial velocity data, the lead author (R.H.N.) first secured, in the springs of 2016, 2017, and 2018, a total of 14 medium resolution (R∼10000 on average) spectra of RZ Com at the DAO using the 1.83 m Plaskett Telescope. This system features a Cassegrain spectrograph fitted with (in this case) the 21181Yb grating (1800 lines/mm and blazed at 5000 Å) which produces a first order linear dispersion of 10 Å/mm. The wavelengths ranged from 5000 to 5260 Å, approximately. A log of observations is given in Table 2 and an eclipse timing diagram, in Figs. 11 and 12 later in the paper. The latter was used to derive the following elements (Eq 1), used for both this photometric data set and also RV phasing:

$$\text{JD (Hel) Min I} = 2458253.6296\ (152) + 0.3385075\ (4) \qquad (1)$$

where the quantities in brackets are the standard errors of the preceding quantities in units of the last digit.

Frame reduction was performed by software RaVeRe (Nelson 2013). See Nelson (2010) and Nelson et al. (2014) for further details. The normalized spectra are reproduced in Fig. 1, sorted by phase (the vertical scale is arbitrary). Note towards the right the strong neutral iron lines (at 5167.487 and 5171.595 Å) and the strong neutral magnesium triplet (at 5167.33, 5172.68, and 5183.61 Å).

Radial velocities were determined using the Rucinski broadening functions (Rucinski 2004, Nelson 2010) as implemented in software Broad25 (Nelson 2013). See Nelson

Table 2: Log of DAO observations.

DAO Image #	Mid Time (HJD−2400000)	Exposure (sec)	Phase at Mid-exp	V_1 (km/s)	V_2 (km/s)
16-1275	57493.7798	2831	0.294	−228.7 (4.9)	133.0 (5.1)
16-1331	57495.9583	3600	0.729	254.1 (2.2)	−94.3 (6.1)
16-1431	57498.6938	3600	0.810	241.6 (2.6)	−89.2 (4.5)
16-1433	57498.7365	3600	0.937	—	−33.0 (2.6)
16-1439	57498.8335	3600	0.223	−232.8 (4.0)	123.4 (4.1)
16.1441	57498.8774	3600	0.353	−173.1 (2.5)	85.3 (2.3)
16-1455	57499.6844	2400	0.737	270.4 (3.0)	−103.5 (3.2)
16-1467	57500.8635	1605	0.220	−235.2 (3.7)	122.4 (4.9)
16-1484	57504.7129	2100	0.592	136.6 (7.1)	−81.4 (4.5)
16-1502	57504.9060	1800	0.162	−203.0 (4.6)	103.4 (3.5)
17-3989	57859.7304	900	0.365	−177.9 (4.9)	116.7 (3.1)
18-5239	58231.8677	1800	0.712	258.7 (3.2)	−102.1 (5.5)
18-5342	58233.9179	1800	0.769	268.7 (2.3)	−101.7 (6.7)
18-5486	58241.8496	1800	0.200	−222.4 (3.9)	114.5 (2.0)

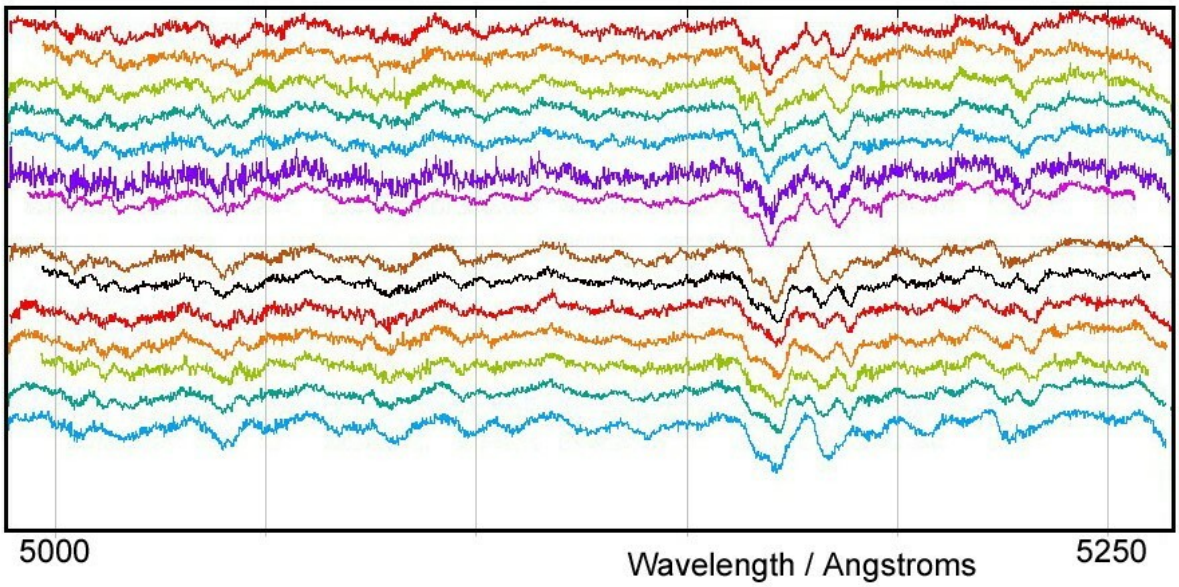

Figure 1. RZ Com spectra at phases 0.162, 0.200, 0.220, 0.223, 0.294, 0.353, 0.365, 0.592, 0.712, 0.729, 0.737, 0.769, 0.810, 0.937 (from top to bottom). Each has been shifted vertically for clarity. The vertical scale is arbitrary.

et al. (2014) for further details. An Excel worksheet (with built-in macros written by him) was used to do the necessary radial velocity conversions to geocentric and back to heliocentric values (Nelson 2014). The resulting RV determinations are also presented in Table 2 along with standard errors (in units of the last digits, enclosed in brackets). The mean rms errors for RV_1 and RV_2 are 6.9 and 11.7 km/s, respectively, and the overall rms deviation from the (sinusoidal) curves of best fit is 12.6 km/s. The best fit yielded the values $K_1 = 249.5(0.7)$ km/s, $K_2 = 114.9(0.9)$ km/s and $V_\gamma = 11.5(0.5)$ km/s, and thus a mass ratio $q_{\rm sp} = K_1/K_2 = m_2/m_1 = 2.17(2)$.

Representative broadening functions, at phases 0.223 and 0.737 are depicted in Figs. 2 and 3, respectively (the vertical scale is arbitrary). Smoothing by a Gaussian filter is routinely done in order to centroid the peak values for determining the radial velocities.

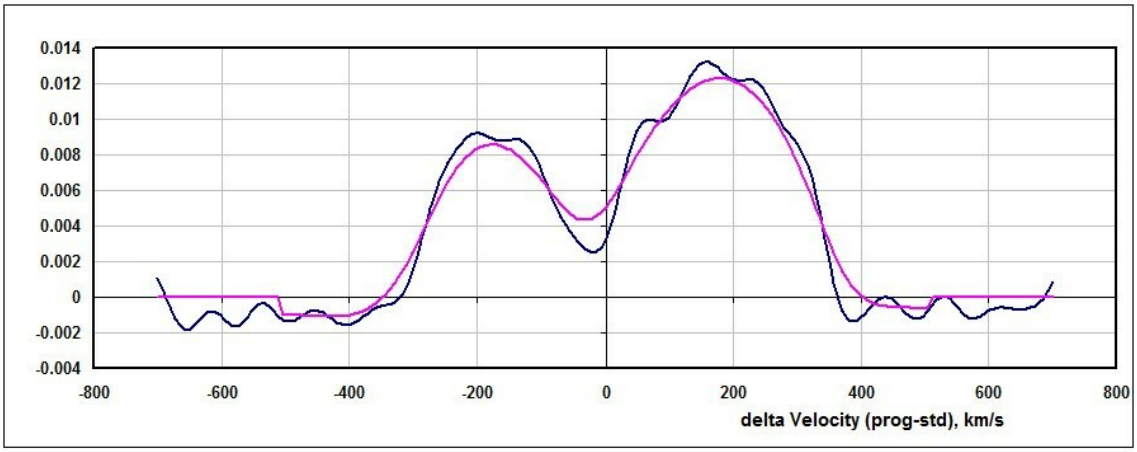

Figure 2. Broadening functions (arbitrary intensity) at phase 0.223—smoothed and unsmoothed.

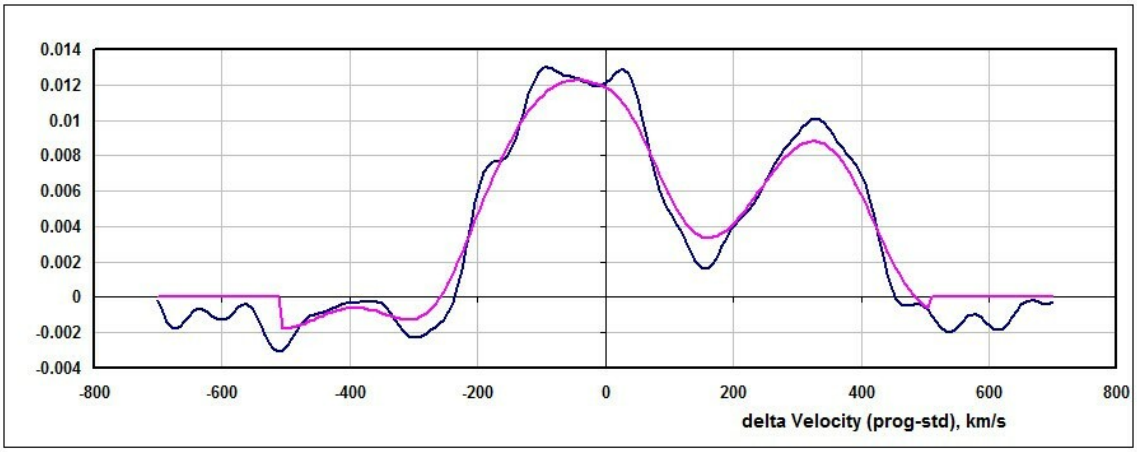

Figure 3. Broadening functions (arbitrary intensity) at phase 0.223—smoothed and unsmoothed.

During four nights in 2018, May 8-18, the lead author took a total of 164 frames in V, 168 in $R_{\rm C}$ (Cousins) and 165 in the $I_{\rm C}$ (Cousins) bands at Desert Blooms Observatory, jointly owned by the authors. Hosted at the San Pedro Observatory complex located

Table 3: Details of variable, comparison and check stars.

Object	TYC	RA (J2000)	Dec (J2000)	V (mag)	$B-V$ (mag)
Variable	1990-2841-1	$12^{\rm h}35^{\rm m}05.06^{\rm s}$	$+23°20'14\farcs0$	10.440 (32)	+0.506 (49)
Comparison	1990-1707-1	$12^{\rm h}34^{\rm m}24.41^{\rm s}$	$+23°27'14\farcs4$	10.571 (57)	0.415 (60)
Check	1990-3503-1	$12^{\rm h}35^{\rm m}18.50^{\rm s}$	$+23°18'11\farcs4$	12.161 (48)	0.537 (56)

near Benson Arizona, the telescope is operated remotely. It consists of a Software Bisque Taurus 400 equatorial fork mount, a Meade LX-200 40 cm Schmidt-Cassegrain optical assembly operating at f/7, a SBIG STT-1603 XME CCD camera (with a field of view $11 \times 18'$), and a filter wheel with the usual B, V, $R_{\rm C}$, and $I_{\rm C}$ filters. For unattended operation, automatic focusing is required owing to the large temperature changes throughout the night (typically +35°to +10°C in late spring).

Standard reductions were then applied (see Nelson et al. 2014 for more details). The variable, comparison, and check stars are listed in Table 3. The coordinates are from the Gaia Catalogue, DR2 and magnitudes are from the APASS catalogue DR9 (Henden, et al. 2009, 2010; Smith et al. 2010).

Radial velocity and light curve analysis was carried out using the 2003 version of the Wilson-Devinney (WD) analysis program with Kurucz atmospheres (Wilson & Devinney, 1971, Wilson et al. 1972, Kurucz 1979, Wilson 1990, Kallrath & Milone 1998, Wilson 1998) as implemented in the Windows front-end software WDwint Nelson (2013). In this process, the first task one faces is to determine the effective temperature of the more luminous component, either from the published spectral type or by some other means. However, as noted in Table 1, the correct classification is unclear. Following the initial classification of Struve & Gratton (1948), which was from actual spectra, and also that of earlier workers, the lead author initiated modelling assuming a spectral type of K0 and an effective temperature T_2 of 5247 ± 150 K based on the calibration of Flower (1996). The choice of this later spectral type was further justified because the computed total mass from the RV curves (assuming 90° inclination) was 1.70 solar masses which nicely corresponds to the tabular value of 1.60 solar masses for a main-sequence G9+K0 pair. Also, because the system was known to be of the W-type subclass (the secondary star in this convention) is the more massive, and can be expected to be more luminous, therefore dominating the classification spectra. Therefore temperature T_2 was held fixed, and temperature T_1 was varied to attain the best fit. (In view of the 'approximate' characterization of Struve & Gratton's classification, the error estimate for T_2 is based on $1\frac{1}{2}$ subclasses.) From the interpolated tables of Cox (2000), a $\log g$ value of 4.476 (cgs) was assumed.

An interpolation program by Terrell (1994), available from Nelson (2013) gave the Van Hamme (1993) limb darkening values; and finally, a logarithmic (LD=2) law for the limb darkening coefficients was selected, appropriate for temperatures < 8500 K (ibid.). The limb darkening coefficients are listed below in Table 4. The values for the second star are based on the later-determined temperature of $T_1 = 5420$ K, $\log g_1 = 4.475$ (and assumed spectral type of G8.) Convective envelopes for both stars were used, appropriate for cooler stars (hence values gravity exponent $g = 0.32$ and albedo $A = 0.5$ were used for each).

From the GCVS 4 designation (EW/KW) and from the shape of the light curve, mode 3 (overcontact) mode was used. Initial fitting was accomplished in LC mode by examining the computed and actual light curves in one passband (V), and adjusting the parameters. Thereafter, convergence using differential corrections (DC) and the method of multiple subsets was reached in a small number of iterations. (See Wilson & Devinney (1971) and

Table 4: Limb darkening values from Van Hamme (1993) for $T_{1,2}$ and $\log g_{1,2}$ as above. The Y band was used in Broglia (1960) and corresponds to a central wavelength of 5300 Angstroms.

Band	x_1	x_2	y_1	y_2
B	0.849	0.851	0.078	0.040
Y	0.795	0.802	0.166	0.150
V	0.782	0.790	0.187	0.156
$R_{\rm C}$	0.713	0.725	0.220	0.198
$I_{\rm C}$	0.628	0.638	0.223	0.207
Bol	0.648	0.647	0.188	0.175

Kallrath & Milone (1998) for an explanation of the method.) The subsets were: (a, V_γ, q, L_1), (T_1, Ω_1), and (i, L_1). Following the recommendation of Binnendijk (1964), a cool spot was added to star 2 near the neck (that is, with a longitude near 0°). At the time, it was believed necessary to add third light, l3.

Following the example of Alton (2010) in which a unified physical light curve model for AC Boo was achieved for no fewer than eight data sets (the light curve differences being due to a time-varying cool spot), the lead author (RHN) proceeded to attempt the same feat using the data sets of Broglia (1960), Xiang & Zhou (2004), Rovithis & Rovithis-Livaniou (1984), and He & Qian (2008). No solution for the third (R&R-L) data set was possible owing to the strange, non-standard shape of the light curves, and to the disparate eclipse depths between light curves. The eclipse depths were comparable in the blue bandpass while, in the visual bandpass, the secondary depth was much shallower. (No known mechanism could account for this disparity, so modelling attempts were abandoned.)

However, comparable fits were achieved for the present data set, and for those of the other three listed above. All spots were placed on star 2 (the more massive) with the exception of the data of Xiang & Zhou (2004), for which the best solution involved no spot. However, there was a snag. When the co-author (KBA) joined the study, he pointed out that, based on his compilation of contemporary colour magnitude differences ($B-V$), the system was likely hotter. Further, the Tycho catalogue Wright, et al., (2003) lists the system as G0Vn, temperature $T_2 = 6030$ K, $\log g_2 = 4.371$. (It was later determined that $T_1 = 6236$ K and $\log g_1 = 4.365$).

No definitive stellar classification supported by UV or-visible spectra is published for RZ Com. Instead, we relied upon an ensemble of $B - V$ colour indices from astrometric and photometric catalogues available through VizieR and those published by Terrell et al. (2012). (See Table 5.) Colour excess was estimated according to Amôres & Lépine (2005) using the companion program ALextin which requires the Galactic coordinates (l,b) and an estimated distance in kpc. The most recent parallax values reported in Gaia DR2 were used (Gaia Collaboration, 2018). Accordingly Alextin iterated a value for interstellar extinction AV, (which led to the corresponding dereddening $E(B-V) = A_V/3.1$ correction for objects within the Milky Way Galaxy and ultimately intrinsic colour $(B - V)_0$). Outliers within the different sources used for $B - V$ colour indices were statistically eliminated from consideration using Grubbs Test (Grubbs 1950) as implemented in the Real Statistics package for Excel. Thereafter the median $(B - V)_0$ result was used to define the effective temperature of the more luminous star and its corresponding spectral class Pecaut & Mamajek (2013). When we used this approach, the adopted effective temperature ($T_{\rm eff2} = 6070$ K) for RZ Com (Table 5) proved to be slightly higher (6070 vs. 5989 K) but within the confidence intervals reported in the Gaia DR2 release of stellar

Table 5: Spectral classification of RZ Com based upon dereddened[a] $(B-V)$ data from various catalogues and surveys.

Catalogue/Survey	$(B-V)_0$	$T_{\rm eff2}$[b]	Spectral Class[C]
Tycho	0.5100	6240	F7V-F8V
2MASS	0.5539	6034	F9V-G0V
SDSS-DR9	0.5154	6216	F7V-F8V
Terrell et al. (2012)	0.5456	6072	F8V-F9V
APASS	0.4996	6280	F6V-F7V
ASCC	0.5506	6047	F8V-F9V

a: $E(B-V) = 0.0074$;
b: $T_{\rm eff2}$ interpolated + spectral class assigned for most luminous star from Pecaut & Mamajek (2013);
c: Median value for $(B-V)_0 = 0.546 \pm 0.008$; $T_{\rm eff2} = 6070 \pm 93$ K; Spectral class = F8V-F9V

Table 6: New times of minima for V500 Cyg obtained in this study.

Band.	x_1	x_2	y_1	y_2
B	0.841	0.825	0.209	0.185
Y	0.781	0.786	0.230	0.200
V	0.721	0.740	0.267	0.258
$R_{\rm C}$	0.681	0.668	0.279	0.272
$I_{\rm C}$	0.568	0.584	0.271	0.264
Bol	0.640	0.644	0.233	0.225

parameters (Andrae et al. 2018).

It could be argued that the orbital phase at which each of the above $(B-V)_0$ observations was taken is unknown, and therefore taking the mean is questionable. However, in view of the fact that the temperatures of each component are shown below to be very close, it is unlikely that the colour indices could vary to any great extent over an orbital cycle, and certainly less than the variations between values displayed above.

Accordingly, revised values from the van Hamme tables for $T_{1,2} = 6276$, 6070 K, $\log g_{1,2} = 4.365$, 4.371 respectively were determined and listed in Table 6.

We will start with the 2018 data sets presented in this paper; the two solutions are presented in Table 7. Owing to the fact that the light curve plots are virtually indistinguishable, only one plot (B) is presented in Fig. 4.

From Mochnacki (1981), the fill-out factor is $f = (\Omega_{\rm I} - \Omega)/(\Omega_{\rm I} - \Omega_{\rm O})$, where Ω is the modified Kopal potential of the system, $\Omega_{\rm I}$ is that of the inner Lagrangian surface, and $\Omega_{\rm O}$, that of the outer Lagrangian surface, was also calculated.

For the most part, the error estimates (for this data set only) are those provided by the WD routines and are known to be underestimated; however, it is a common practice to quote these values and we do so here. Also, estimating the uncertainties in temperatures T_1 and T_2 is somewhat problematic. A common practice is to quote the temperature difference over–say–one spectral sub-class. assuming that the classification is good to one spectral sub-class, (the precision being unknown in this case). In addition, various different calibrations have been made Flower (1996) and Pecaut & Mamajek (2013), and classification is $\pm$ one sub-class, an uncertainty of $\pm$ 200 K to the absolute temperatures of each, would be reasonable. (The modelling error in temperature T_1, relative to T_2, is indicated by the WD output to be much smaller, around 9 K.)

Trials were also run with the spot on the neck side of star 1 (the hotter star); however, all trials resulted in residuals higher by about 5%. Also, starting with solution B ($T_2 =$

Table 7: Wilson-Devinney parameters for the present dataset.

WD Quantity	Sol'n A	Sol'n B	Error	Unit
Temperature, T_1	5420	6276	200	K
Temperature, T_2	5257	6070	[fixed]	K
$q = m_2/m_1$	2.174	2.179	0.009	—
Potential, $\Omega_1 = \Omega_2$	5.396	5.393	0.010	—
Inclination, i	86.3	86.8	0.6	degrees
Fill-out factor, f_1	0.100	0.11	0.01	—
Semi-major axis, a	2.49	2.49	0.02	$R_\odot$
System RV, V_γ	12.4	12.4	1.4	km/s
Phase shift	0.0021	0.0021	0.0001	—
L_3 (V)	0.021	—	0.003	—
L_3 (R_C)	0.015	—	0.003	—
L_3 (I_C)	0.009	—	0.004	—
$L_1/(L_1 + L_2)$ (V)	0.367	0.364	0.001	—
$L_1/(L_1 + L_2)$ (R_C)	0.361	0.359	0.001	—
$L_1/(L_1 + L_2)$ (I_C)	0.357	0.355	0.001	—
Spot co-latitude	48	47	5	deg
Spot longitude	10	9.1	2	deg
Spot radius	24.9	23.7	0.5	deg
Spot temp. factor	0.912	0.886	0.009	—
r_1 (pole)	0.3017	0.3024	0.0011	orb. rad.
r_1 (side)	0.3160	0.3168	0.0014	orb. rad.
r_1 (back)	0.3544	0.3560	0.0024	orb. rad.
r_2 (pole)	0.4293	0.4303	0.0009	orb. rad.
r_2 (side)	0.4586	0.4599	0.0012	orb. rad.
r_2 (back)	0.4894	0.4910	0.0016	orb. rad.
$\Sigma\omega^2_{\rm res}$	0.0399	0.0393	—	—

6070 K) further trials were run with third light, however they did not improve the fit. An effort was made to go back to test the idea that solution A could be improved by deleting third light. A number of trials were run with no success. In view of the fact that solution B ($T_2 = 6070$ K) of is considered to be the optimum solution, there seemed to be no point in pursuing the matter further. The question then arises as to why we include Solution A at all. The answer is that it can serve as a cautionary tale to modellers in that different parameters can lead to nearly identical residuals and identical plots. In the case of AR CrB, this effect is illustrated more rigorously after adjusting the effective temperature of the more luminous star by as much as 3σ (Alton & Nelson 2018). It is the task of the modeller to sort out the best values based on external criteria.

The light curve data and the fitted curves from this paper are depicted in Fig. 4 (from top to bottom: V, R_C, and I_C), shifted by 0.1 flux units. The residuals in the sense (observed-calculated) are also plotted, shifted downward, and from each other by 0.05 units.

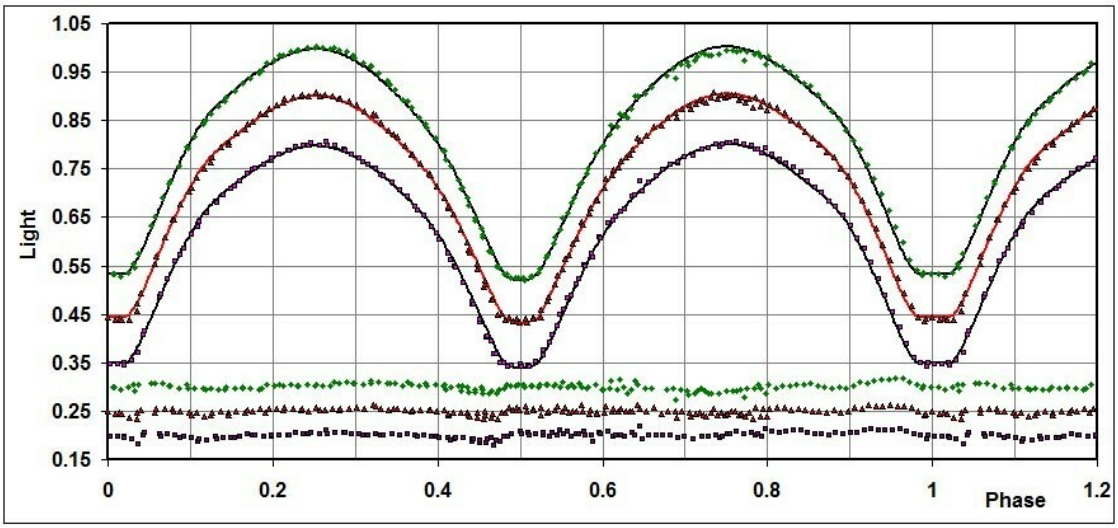

Figure 4. (top to bottom) V, R_C, and I_C light curves for RZ Com (this paper) – Data, WD fit, residuals. For clarity, the top three curves were offset by 0.10 divisions, while the bottom three, by 0.05 divisions.

Next, the data sets from Broglia (1960) were modelled, starting with data set 1. The solutions from this paper, along with those in Wilson & Devinney (1973), are presented in Table 8.

Next, the second dataset from Broglia (1960) was modelled. The solutions from this paper, along with those in Wilson & Devinney (1973), are presented in Table 9.

This time, the plots for both data sets are combined and presented in Fig. 5. Once again, plots for the two solutions are indistinguishable; hence only one figure is required.

Next, the data set from Xiang & Zhou (2004) was modelled. The problem here is that, visually, one can see there is significantly greater scatter in the data from phase 0.8 to 1.0. An analysis of the rms deviations for the curves of best fit using bins of 0.05 phase revealed that weights of 0.1 for phase 0.8 to 1.0, and 1 everywhere else were appropriate. With this modification, modelling proceeded.

Table 8: Wilson-Devinney parameters for the first dataset of Broglia (1960).

WD Quantity.	W&D 1973	Sol'n A	Sol'n B	Error	Unit
Temperature, T_1	5500	5420	6307	19	K
Temperature, T_2	5564	5257	6070	[fixed]	K
$q = m_2/m_1$	2.292 (30)	2.185	2.22	0.02	—
Potential, $\Omega_1 = \Omega_2$	5.618 (54)	5.396	5.44	0.03	—
Inclination, i	86.04 (51)	85.7	86.0	1.1	deg.
Fill-out factor, f_1	0.042	0.12	0.15	0.02	—
Semi-major axis, a	na	2.49	2.48	0.02	$R_\odot$
System RV, V_γ	na	12.4	12.2	1.2	km/s
Phase shift	—	0.0006	0.0006	0.0004	—
L_3 (Y)	—	0.015	—	—	—
$L_1/(L_1 + L_2)$ (Y)	na	0.366	0.366	—	—
Spot co-latitude	—	76	80	10	deg
Spot longitude	—	4	3.5	8	deg
Spot radius	—	27	26.6	4	deg
Spot temp. factor	—	0.9596	0.946	0.016	—
r_1 (pole)	0.2924 (44)	0.3026	0.3023	0.0026	orb. rad.
r_1 (side)	0.3056 (52)	0.3172	0.3169	0.0033	orb. rad.
r_1 (back)	0.3403 (82)	0.3567	0.3573	0.0058	orb. rad.
r_2 (pole)	0.4287 4(2)	0.4310	0.4333	0.0022	orb. rad.
r_2 (side)	0.4574 (55)	0.4608	0.4636	0.0029	orb. rad.
r_2 (back)	0.4859 (71)	0.4921	0.4952	0.0040	orb. rad.
$\Sigma\omega^2_{\rm res}$	—	0.0046	0.0046	—	—

Table 9: Wilson-Devinney parameters for the second dataset of Broglia (1960).

WD Quantity..	W&D 1973	Sol'n A	Sol'n B	Error	Unit
Temperature, T_1	5500	5470	6325	14	K
Temperature, T_2	5552	5257	6070	[fixed]	K
$q = m_2/m_1$	2.394 (20)	2.19	2.20	0.04	—
Potential, $\Omega_1 = \Omega_2$	5.869 (40)	5.40	5.40	0.09	—
Inclination, i	85.72 (31)	86.3	86.3	0.6	degrees
Fill-out factor, f_1	-0.059	0.12	0.13	0.03	—
Semi-major axis, a	na	2.49	2.49	0.02	$R_\odot$
System RV, V_γ	na	12.4	12.4	1.1	km/s
Phase shift	—	0.0001	0.0001	0.0003	—
L_3 (Y)	—	0.013	—	—	—
$L_1/(L_1 + L_2)$ (Y)	na	0.376	0.377	—	—
Spot co-latitude	—	115	115	10	deg
Spot longitude	—	0	0	8	deg
Spot radius	—	27.0	27	4	deg
Spot temp. factor	—	0.971	0.971	0.016	—
r_1 (pole)	0.2805 (30)	0.3030	0.3038	0.0083	orb. rad.
r_1 (side)	0.2918 (35)	0.3177	0.3186	0.0101	orb. rad.
r_1 (back)	0.3211 (52)	0.3577	0.3596	0.0176	orb. rad.
r_2 (pole)	0.4240 (29)	0.4317	0.4331	0.0074	orb. rad.
r_2 (side)	0.4509 (37)	0.4617	0.4635	0.0098	orb. rad.
r_2 (back)	0.4761 (47)	0.4933	0.4955	0.0132	orb. rad.
$\Sigma\omega^2_{\rm res}$	—	0.0077	0.0040	—	—

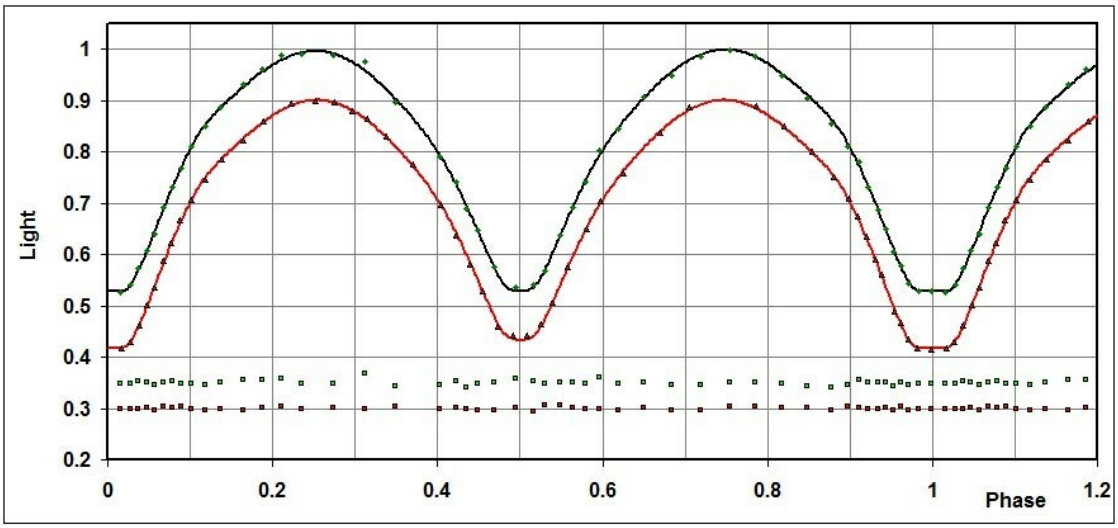

Figure 5. *Y* light curves (1 & 2) of Broglia (1960) – Data, our WD fits, residuals. For clarity, the curves have been offset as in Fig. 4.

The two solutions from this paper, along with those from Xiang & Zhou (2004), are presented in Table 10.

This time, there is a significant difference in the plots for solutions A & B; hence both are presented, in Figs. 6 and 7.

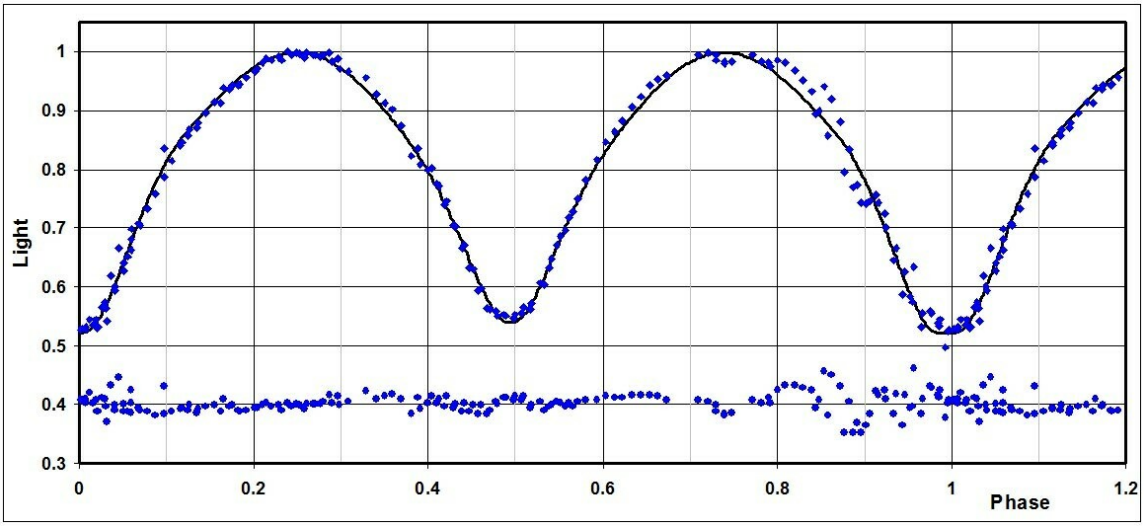

Figure 6. *B* light curve of Xiang & Zhou (2004): – Data, our WD fit A, (residuals offset)

And, lastly, we modelled the data of He & Qian (2008). As the analysis occurred late in the paper writing, we did not attempt a fit using the lower temperatures, but merely started with the parameters obtained from the other datasets. To our surprise, the spot had moved significantly in longitude. The results are listed in Table 11.

The light curve data from He & Qian (2008) and the fitted curves from this paper are depicted in Fig. 8 (from top to bottom: *B* and *V*), shifted by 0.1 flux units. The

Table 10: Wilson-Devinney parameters for the dataset of Xiang & Zhou (2004).

WD Quantity...	Xiang & Zhou Tbl 5	Xiang & Zhou Tbl 6	Sol'n A	Sol'n B	Error	Unit
Temperature, T_1	4900	4900	5425	6289	18	K
Temperature, T_2	4842	4802 (9)	5257	6070	[fixed]	K
$q = m_2/m_1$	2.226 (13)	0.772 (9)	2.19	2.20	0.02	—
Potential, $\Omega_1 = \Omega_2$	5.267 (15)	3.330 (14)	5.39	5.40	0.02	—
Inclination, i	79.67 (28)	78.40 (31)	83.2	81.6	0.5	degrees
Fill-out factor, f_1	na	na	0.13	0.12	0.01	—
Semi-major axis, a	na	na	2.49	2.51	0.02	$R_\odot$
System RV, V_γ	na	na	12.4	12.2	1.1	km/s
Phase shift	na	na	-0.0056	-0.0055	0.0005	—
L_3 (B)	—	—	0.053	—	—	—
$L_1/(L_1 + L_2)$ (B)	0.3699 (31)	0.3833 (11)	0.378	0.376	0.002	—
r_1 (pole)	0.3090 (8)	0.4051 (14)	0.3039	0.3039	0.0027	orb. rad.
r_1 (side)	0.3246 (10)	0.4376 (17)	0.3187	0.3188	0.0034	orb. rad.
r_1 (back)	0.3676 (17)	0.4376 (17)	0.3595	0.3599	0.0062	orb. rad.
r_2 (pole)	0.4327 (17)	0.3403 (34)	0.4327	0.4334	0.0018	orb. rad.
r_2 (side)	0.4634 (23)	0.3573 (43)	0.4630	0.4639	0.0025	orb. rad.
r_2 (back)	0.4967 (33)	0.3921 (69)	0.4949	0.4960	0.0036	orb. rad.
$\Sigma\omega^2_{\rm res}$	0.003617	0.004221	0.0091	0.0088	—	—

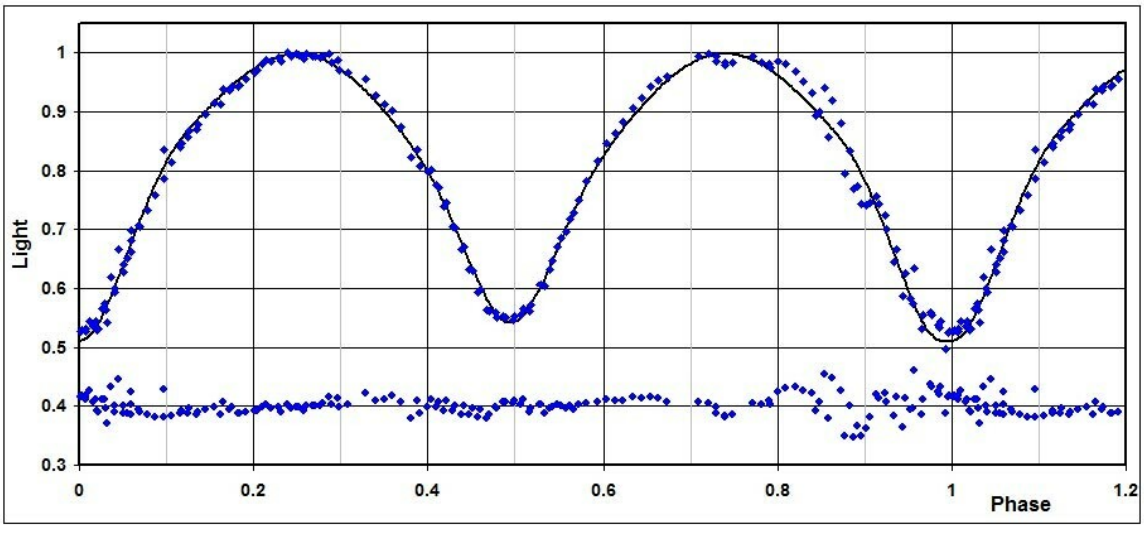

Figure 7. B light curve of Xiang & Zhou (2004): our solution B – Data, our WD fit B, (residuals offset)

Table 11: Wilson-Devinney parameters for the dataset of He & Qian (2008).

WD Quantity....	He & Qian 2008	Our sol'n	Error	Unit
Temperature, T_1	5000	6267	13	K
Temperature, T_2	4900 (8)	6070	—	K
$q = m_2/m_1$	2.351 (31)	2.174	0.062	—
Potential, $\Omega_1 = \Omega_2$	5.620 (45)	5.38	0.19	—
Inclination, i	81.4 (4)	84.9	0.4	degrees
Fill-out factor, f_1	0.201 (74)	0.11	0.01	—
Semi-major axis, a	—	2.49	0.03	$R_\odot$
System RV, V_γ	—	12.4	1.8	km/s
Phase shift	—	-0.0005	0.0003	—
$L_1/(L_1 + L_2)$ (B)	0.3471 (37)	—	—	—
$L_1/(L_1 + L_2)$ (V)	0.3545 (41)	0.364	0.001	—
r_1 (pole)	0.2971 (45)	0.3026	0.0177	orb. rad.
r_1 (side)	0.3113 (55)	0.3171	0.0215	orb. rad.
r_1 (back)	0.3512 (98)	0.3664	0.0362	orb. rad.
r_2 (pole)	0.4371 (37)	0.4302	0.0163	orb. rad.
r_2 (side)	0.4682 (49)	0.4598	0.0215	orb. rad.
r_2 (back)	0.4990 (67)	0.4910	0.0287	orb. rad.
$\Sigma\omega^2_{\rm res}$	0.00101	0.0235	—	—

residuals in the sense (observed-calculated) are also plotted, shifted downward, and from each other by 0.05 units.

The radial velocities are plotted in Fig. 9. Three-dimensional representations created using Binary Maker 3 (Bradstreet, 1993) for each of the studied epochs are shown in Fig. 10. (The crosses represent the centres of mass of the individual stars and of the system as a whole.)

From the WD output parameters we calculated the fundamental properties corresponding to each of the $T_2 = 6070$ K solutions; the results are listed in Table 12. Most of the errors are output or derived estimates from the WD routines. The values from Hilditch et al. (1988) as reported in Yildiz & Doğan (2013; hereafter Y&D) are included in column 2 for comparison.

Also included for comparison in Table 12 are the interpolated values from Pecaut & Mamajek (2013) for single main-sequence stars (as a function of temperature), in column 8. As noted in Y&D, the values for the more massive star m_2 (in our convention) are not far off the main sequence values. On the other hand, the less massive star is either underluminous for a star of its temperature (and therefore spectral class), or is over-luminous for a main sequence star of the same mass. From the interpolated tables of Pecaut & Mamajek (2013), the primary of mass 0.57 $M_\odot$ should have a luminosity of 0.093 $L_\odot$. See the concluding remarks for more discussion on this point.

To determine the distances r for the present data in the last row, we proceeded as follows: First the WD routine gave the absolute bolometric magnitudes of each component; these were then converted to the absolute visual (V) magnitudes of both, $M_{V,1}$ and $M_{V,2}$, using the bolometric corrections BC $= -0.06$ and -0.08 for stars 1 and 2 respectively. The latter were taken from tables constructed from Pecaut & Mamajek (2013). The absolute V magnitude was then computed in the usual way, getting $M_V = 3.84 \pm 0.03$ magnitudes.

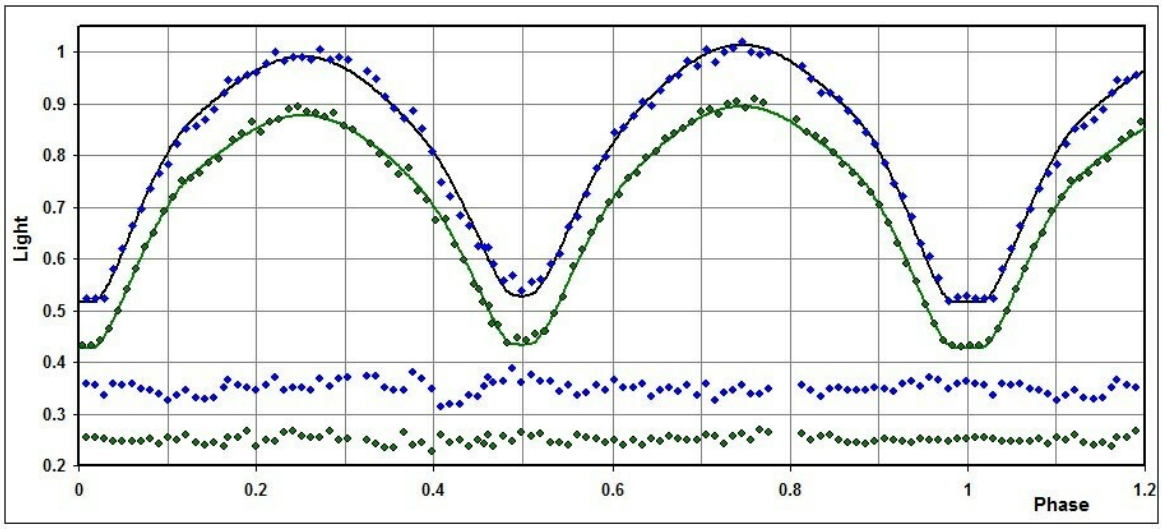

Figure 8. B and V light curves of He & Qian (2008) – Data, our WD fits, residuals. For clarity, the curves have been offset as in Fig. 4.

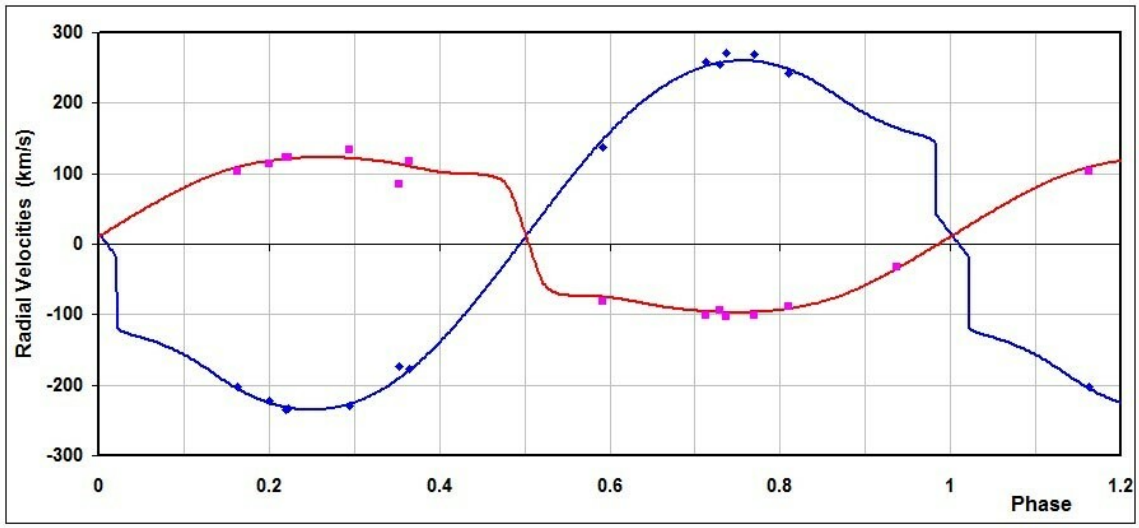

Figure 9. Radial velocity curves for RZ Com (this paper) – Data and WD Fit.

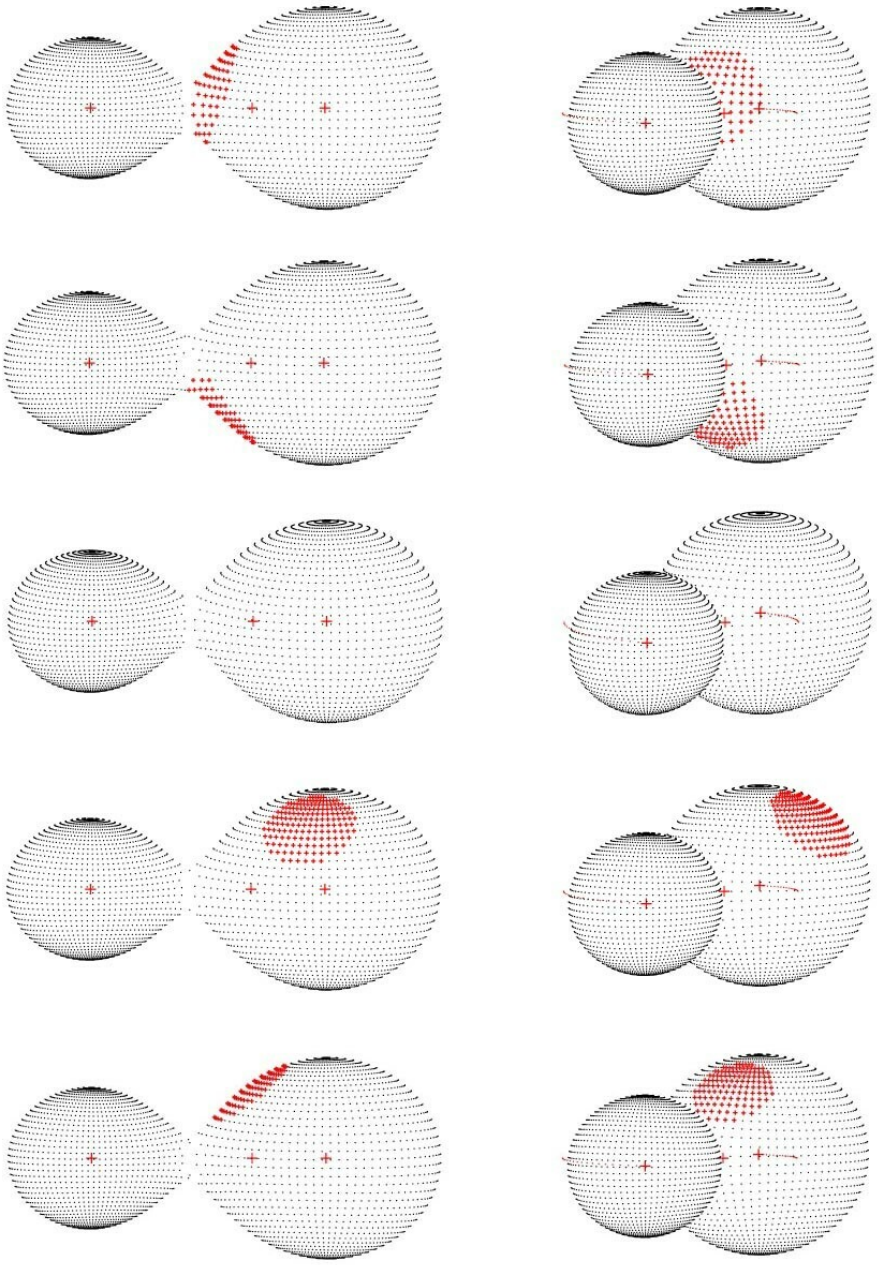

Figure 10. Binary Maker 3 representations of the system. Top to bottom: Broglia (1960) data set 1, Broglia (1960) data set 2, Xiang & Zhou (2004), He & Qian (2008), dataset from this paper (2018). Left to right: phase 0.25, phase 0.42.

Table 12: Fundamental parameters. Errors are for the data set of this paper only.

Quantity	Hilditch (1988)	Broglia 1	Broglia 2	Xiang-Zhou	He & Qian	This dataset	Error	Cox (2000)	unit unit
Temp., T_1	6457 (298)	6307	6325	6289	6267	6246	200	—	K
Temp., T_2	6166 (284)	6070	6070	6070	6070	6070	[fixed]	—	K
Mass, m_1	0.55 (4)	0.557	0.570	0.582	0.574	0.573	0.007	1.55	$M_\odot$
Mass, m_2	1.23 (9)	1.239	1.253	1.282	1.248	1.249	0.009	1.16	$M_\odot$
Radius, R_1	0.78 (2)	0.81	0.82	0.83	0.82	0.82	0.01	1.22	$R_\odot$
Radius, R_2	1.12 (3)	1.16	1.16	1.17	1.15	1.15	0.01	1.11	$R_\odot$
$M_{\rm bol,1}$	—	4.86	4.82	4.83	4.87	4.87	0.01	3.77	mag
$M_{\rm bol,2}$	—	4.26	4.25	4.41	4.26	4.26	0.01	4.12	mag
$\log g_1$	—	4.36	4.36	4.37	4.37	4.37	0.01	4.36	cgs
$\log g_2$	—	4.40	4.41	4.41	4.41	4.41	0.01	4.37	cgs
Luminosity, L_1	0.93 (15)	0.94	0.97	0.96	0.93	0.93	0.03	2.04	$L_\odot$
Luminosity, L_2	1.62 (26)	1.63	1.64	1.68	1.63	1.63	0.03	1.16	$L_\odot$
Distance, r	—	204	204	204	201	204	5	—	pc

The apparent magnitude in the V passband was $V = 10.44 \pm 0.03$, taken from the APASS catalogue (Henden et al., 2009, 2010; Smith et al. 2010). In order to check that the values were obtained at the correct phase (i.e., near phase 0.25 or 0.75—when the flux from both stars was maximum), photometry at these phases was analysed using the comparison star and its V magnitude of 10.571 (57), also taken from the APASS catalogue. The result: $V = 10.437$ (5) where the error stated is the standard error of the mean; including the error in the comparison magnitude, resulted in $V = 10.44$ (6).

Because of the system's high galactic latitude (+84.7°), and as we will see, its close proximity, interstellar absorption, A_V may be ignored initially. Therefore using the standard relation (Eq 2) with $A_V = 0$, we calculated a value for the distance as $r = 209$ pc:

$$r = 10^{0.2(V - Mv - A_V + 5)} \text{ parcsec} \qquad (2)$$

Galactic extinction was obtained from a model by Amôres & Lépine (2005). The code available in IDL (and converted by the author to a Visual Basic routine) assumes that the interstellar dust is well mixed with the dust, that the galaxy is axi-symmetric, that the gas density in the disk is a function of the Galactic radius and of the distance from the Galactic plane, and that extinction is proportional to the column density of the gas, Using Galactic coordinates of $l = 257.7516°$ and $b = +84.7047°$ (SIMBAD), and the initial distance estimate of $d = 0.208$ kpc, a value of $A_V = 0.070$ magnitude was determined. A further iteration revealed little change in A_V. Substitution into (2) gave $r = 202$ pc. Similar calculations were carried out for the other datasets.

However, there was a problem. The value derived from the Schlegel dust maps (Schlegel et al. 1998)[1], and including the factor sin(galactic latitude) is $A_V = 0.045$ mag. As this value pertains to the absorption all the way through the Galactic arm (a distance of approximately 0.3 kpc), the value from Amôres & Lépine appears to overestimate interstellar extinction in this region of the sky. If we take 2/3 of the Schlegel value ($2/3 \times 0.045$) we get $A_V = 0.03$ mag. Substitution into (2) gave $r = 206$ pc, close to the above value. Therefore we adopt the mean of the two computed values, 204 pc. The same procedure was used with the other datasets in Table 12.

The errors were assigned as follows: $\delta M_{\rm bol,1} = \delta M_{\rm bol,2} = 0.02$, $\delta BC_1 = \delta BC_2 = 0.005$ (the variation of 1/2 spectral sub-class), $\delta V = 0.04$, all in magnitudes. Combining the errors rigorously (i.e., by adding the variances) yielded an estimated error in r of 5 pc.

[1] available at: `http://www.astro.princeton.edu/~schlegel/dust/data/data.html`, by Schlegel, D. J., Finkbeiner, D. P., Krigel, A. (2013)

Table 13: New times of minima for RZ Com obtained in this study.

Min (Hel)−2400000	Type	Error (days)
58169.8508	II	0.0002
58246.8611	I	0.0004
58250.7519	II	0.0002
58253.7986	II	0.0002

Table 14: LiTE parameters from various sources.

LiTE Quantity	Qian &He 2005	He & Qian 2008	Nelson et al. 2016	This work	Unit
Period, P_3	44.8 (7)	45.1 (6)	41.4 (5)	41.4 (7)	years
Amplitude, A	0.0058 (5)	0.0065 (1)	0.0063 (3)	0.0063 (4)	days
Eccentricity, e_3	0	0	0.30 (11)	0.30 (12)	—
Arg. Periastr., ω_3	260 (7)	278 (7)-	472 (25)	472 (35)	degrees
Periastron time	—	—	42744 (1790)	42772 (2643)	HJD−2400000
$a_1 2 \sin i$	1.00 (9)	1.12 (2)	1.09 (6)	1.10 (6)	AU
f (m_3)	0.00051 (13)	—	0.00076 (12)	0.00077 (14)	$M_\odot$
dP/dt (1-2 pair)	4.12	3.97	3.86 (8)	3.84 (2)	10-8 d/yr

The Gaia DR2 catalogue lists, for RZ Com, a parallax of 4.898 ± 0.088 mas. This translates to a distance of 203.1 ± 3.7 pc, consistent with all our distance estimates.

Four new times of minima emerged from the observations; these are reported in Table 13. Each is the mean of three values (one for each filter). For each filter, five methods of minimum determination, as implemented in software Minima23 Nelson (2013) were used: the digital tracing paper method, bisection of chords, sliding integrations (Ghedini 1982), curve fitting using five Fourier terms, and Kwee and van Woerden (Kwee & Woerden 1956, Ghedini 1982). There was no significant difference between corresponding values for the different filters. Because, in the literature, many (or perhaps most) error estimates can be shown to be low (sometimes unrealistically so), the estimated errors were taken as double the standard deviations of the various determinations. Also, a minimum error value of 0.0002 days was adopted for the same reason.

The period behaviour of this system is very interesting, and was earlier examined in Nelson et al. (2016). An eclipse timing difference (O–C) plot using the same timings dating from 1927 but updated with more recent points was used. Earlier fits are due to Qian & He (2005) and He & Qian (2008). As with Nelson et al. (2016), derivations of the light time effect (LiTE) using relations from Irwin (1952, 1959), resulted in a good fit. Standard weighting was used: pg = 0.2, vis = 0.1, and PE, CCD = 1.0.

As the reader will see in Table 14, parameters in the updated fit differ only slightly (if at all) from Nelson et al. (2016).

The eclipse timing difference (O–C) plot with all available timings together with the latest LiTE fit is depicted in Fig. 11.

From the definition of the mass function given in equation 3:

$$f(m_3) = (m_3 \sin i')^3/(m_1 + m_2 + m_3)^2 \quad (3)$$

and the value from this work, we were able to estimate a value for m_3. Assuming that the inclination i' of the putative third star orbit is the same as that of the eclipsing pair (viz. 85°), we calculated mass m_3 by iteration, obtaining the value $m_3 = 0.144$ (8) $M_\odot$. From the tables of Cox (2000) for main sequence stars, we read that the luminosity would be 0.0009 $L_\odot$, which is far too faint to be of any consequence to the modelling process here.

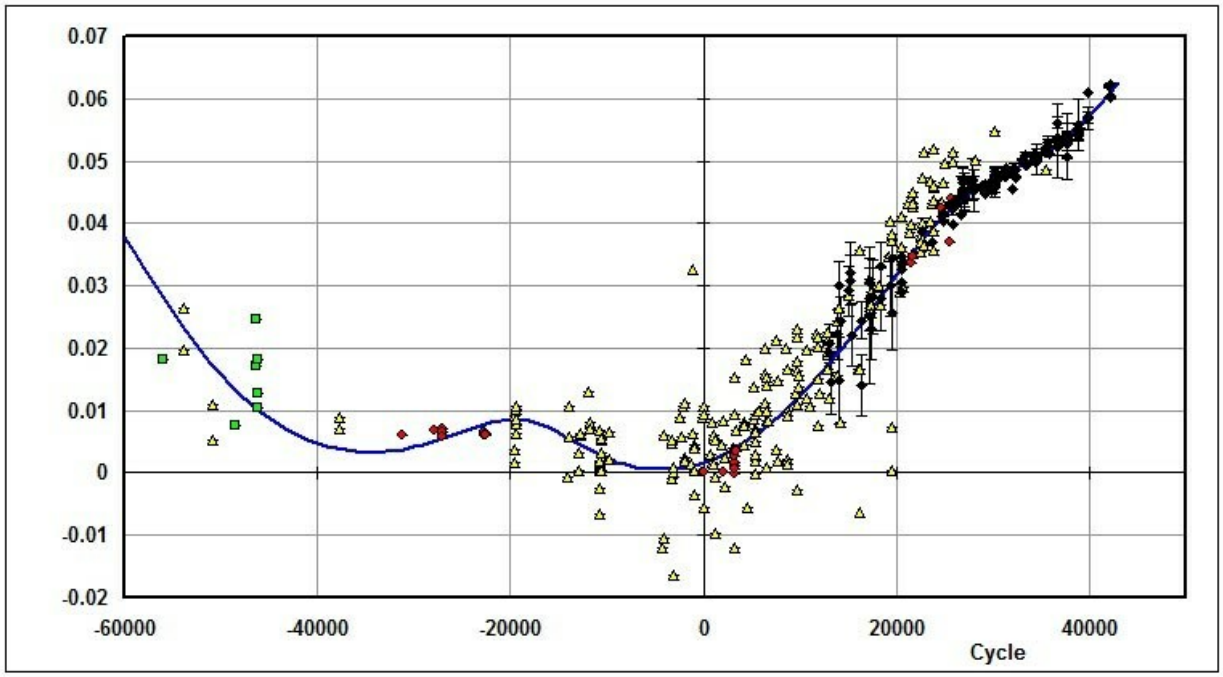

Figure 11. RZ Com – eclipse timing (O–C) diagram with LiTE fit (see text). [Note: (green) squares = photographic; (yellow) pyramids = visual; (red) circles = photoelectric; and (black) diamonds = CCD.] Elements used to generate this plot are given in Equation 4.

$$\text{JD (Hel) Min I} = 2443967.9371\ (29) + 0.33850604\ (5)\ \text{E} \tag{4}$$

In order to phase the photometric and radial velocity curves correctly, a different set of elements, applying to the interval over which the data were taken, was required. For the present data set, timings from 2014-2018 were used with the exclusion of all else; the results of the fit are shown in Fig. 12.

This resulted in the elements of Equation 5 given below. These elements were used for all phasing of the RV and present photometric data.

$$\text{JD (Hel) Min I} = 2458253.6296\ (29) + 0.3385075\ (5)\ \text{E} \tag{5}$$

Similar fits were used for the other data sets. Elements for the Broglia (1960) photometric data were:

$$\text{JD (Hel) Min I} = 2458253.5711\ (12) + 0.33850598\ (5)\ \text{E} \tag{6}$$

and those for the Xiang & Zhou (2004) photometric data:

$$\text{JD (Hel) Min I} = 2458253.6628\ (29) + 0.3385088\ (5)\ \text{E} \tag{7}$$

Elements were not required for the data of He & Qian (2008) as their reported data were already phased.

The Excel file for the eclipse timing data and analysis for this system (and for many others) is available at Nelson (2016).

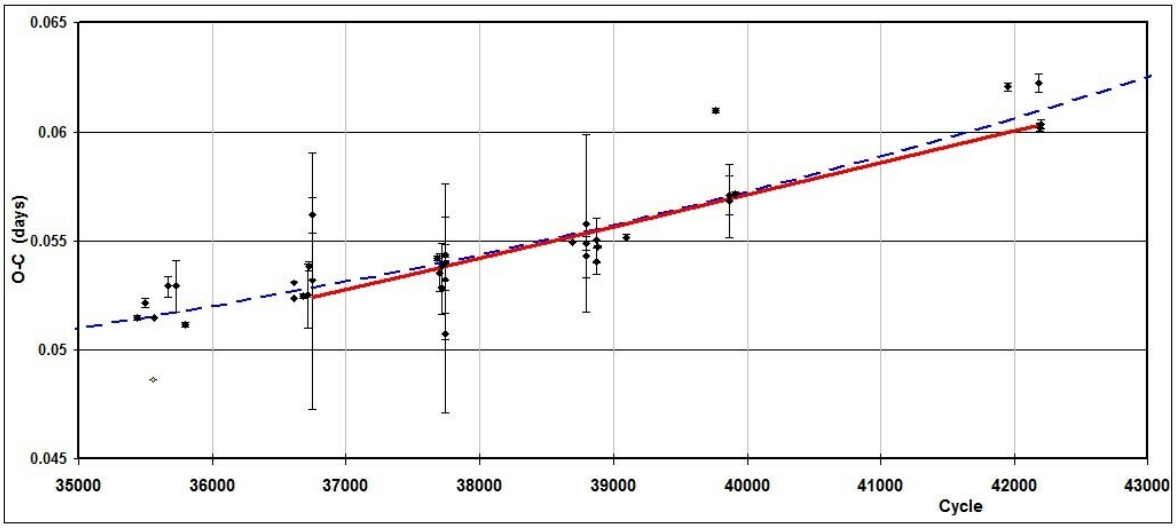

Figure 12. RZ Com – eclipse timing (O–C) diagram with LiTE fit (dashed line) and linear fit for the range

Further, once the LiTE fit was achieved, it was now possible to plot the residuals (see Fig. 13); that is the O–C values minus the LiTE component (see Nelson et al. 2016 for details).

The equation of the line of best fit is:

$$O - C = 0.0078\ (8) + 6.6\ (1) \times 10^{-7}\ \mathrm{E} + 1.79(0.12) \times 10^{-11}\ \mathrm{E}^2 \tag{8}$$

From the quadratic coefficient, c2 one calculates the intrinsic rate of period change, dP/dt by:

$$dP/dt = 2c_2 365.24/P = 3.86\ (21) \times 10^{-8}\ \mathrm{days/year} \tag{9}$$

where P = the orbital period of the eclipsing pair.

If this (constant) rate of period change is due to conservative mass exchange, we may calculate this rate by (see Nelson et al. 2016 for references):

$$dm_1/dt = [3P(1/m_2 - 1/m_1)]^{-1}\, dP/dt \tag{10}$$

Substituting the mean stellar masses for m_1 and m_2 from Table 12, we obtained the value $dm1/dt = -4.1\ (3) \times 10^{-8}\ \mathrm{M}_\odot$/year which means that (as is often the case) the less massive star is losing mass to its companion.

However, it is not clear that the condition of conservative mass transfer is valid. Y&D concluded that, for overcontact binaries, only 34 per cent of the mass from the lesser massive star is transferred to the more massive one. Hence, the value for dm_1/dt should be treated with caution. See also Yildiz (2014).

In conclusion, we have shown that–contrary to the conclusion of Wilson & Devinney (1973), but in agreement with the results of Hilditch et al. (1988), and He & Qian (2008)–this binary system is a W-type overcontact binary with a low fillout factor. Our finding is buttressed by the fact that all our attempts to model the light curve data of this paper as a detached or semi-detached system have failed. Changes recommended in differential corrections always drove the model into mode 3 (overcontact binary).

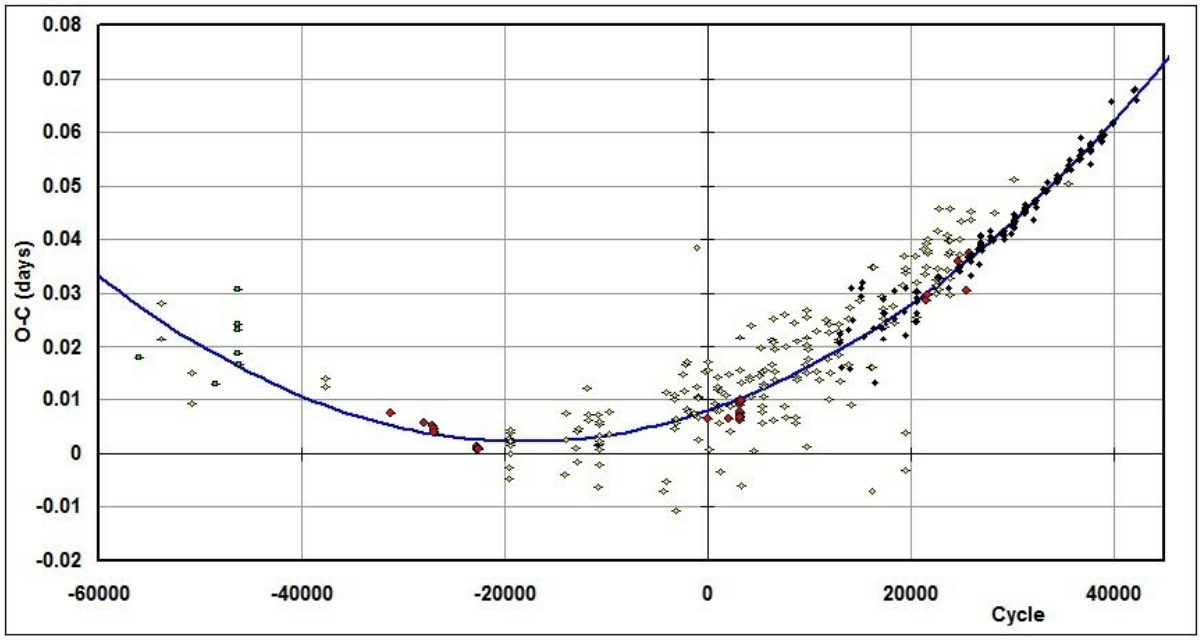

Figure 13. The O–C values for RZ Com minus the LiTE component with the quadratic of best fit.

With our values for the fill-out factor ranging from 0.10 to 0.13, that makes the system a slightly-overcontact binary, typical of the W-types (Rucinski 1974, Kallrath & Milone 1998). Further, our reciprocal mass ratio q′ $= m_1/m_2 = 1/q = 0.45$ lies in the middle of the 'moderate' range ($0.4 < q' < 0.6$), typical of the W-type (Kallrath & Milone 1998).

We also found unified solutions for all the datasets (except as noted) spanning some 60 years. A cool spot on the more massive star accounted for the changes in the light curves over time, giving plausible spot configurations. There appears to be an easy progression between the two data sets of Broglia, and also between the datasets of He & Qian, and with ours. There seemed to be no spot at the epoch of the Xiang & Zhou dataset, however, the higher scatter in their dataset does not allow one to be sure. RZ Com is probably a good candidate for extensive coverage in order to map in detail the progression of the spot.

From Table 12, it is evident that star 1 is underluminous compared to a main sequence star of the same temperature or spectral type, or that it is undermassive for its spectral type the two conditions are equivalent (because a less massive star would have a smaller radius, a smaller emitting area, and hence a lower luminosity). This discrepancy was also noted in Wilson & Devinney (1973) who found 'masses which seem incompatible with their position on the H-R diagram'. However, there is an explanation. According to the calculations of Y&D, the initial mass of the hotter star of RZ Com (designated the primary here, the secondary in Y&D), was much higher, starting at 1.58 $M_\odot$ followed by a period of mass exchange, ending up with a mass of 0.55 $M_\odot$, not far from our value of 0.573(7) $M_\odot$. Again, according to Y&D, the luminosity of our primary (m_1) would depend as much on its initial mass as it does on its present mass, hence the excess luminosity [for its mass]. Y&D also determined the main-sequence age to be 2.09 Gyr.

Acknowledgements: It is a pleasure to thank the staff members at the DAO (Dmitry Monin, David Bohlender, and the late Les Saddlmyer) for their usual splendid help

and assistance. Many thanks are also due to the San Pedro Observatory resident astronomer/technician, Dean Salman for his tireless help. Much use was made of the VizieR search tool along with the SIMBAD and O–C Gateway (B.R.N.O.)[2] databases. This research has made use of the APASS database, located at the AAVSO web site. Funding for APASS has been provided by the Robert Martin Ayers Sciences Fund.

References:

Alton, K. B., 2010, *JAVSO*, **38**, 57
Alton, K. B., Nelson, R. H., 2018, *MNRAS*, **479**, 3197 DOI
Amôres, E. B., Lépine, J. R. D., 2005, *AJ*, **130**, 659 DOI
Andrae,R., Fouesneau, M., Creevey, O., et al., 2018, *A&A* (arXiv: 1804.09374)
Batten A. H., Fletcher J. M., MCarthy D. G., 1989, *Publ. DAO*, **17**
Binnendijk, L., 1964, *AJ*, **69**, 154 DOI
Binnendijk, L., 1970, *Vistas in Astronomy*, **12**, 217 DOI
Bradstreet, D. H., 1993, "Binary Maker 2.0 – An Interactive Graphical Tool for Preliminary Light Curve Analysis", in Milone, E.F. (ed.) Light Curve Modelling of Eclipsing Binary Stars, pp 151-166 (Springer, New York, N.Y.) DOI
Broglia, P., 1960, *Contributi Milano-Merate*, **165**
Gaia Collaboration, 2018, *A&A*, **616**, 1 DOI
Cox, A. N., ed., 2000, *Allen's Astrophysical Quantities*, 4th ed., (Springer, New York, NY) DOI
Flower, P. J., 1996, *ApJ*, **469**, 355 DOI
Gaposchkin, S., 1932, *VeBB*, **9**, 1
Gaposchkin, S., 1938, *Variable Stars* (Harvard Monograph No. 5, Harvard U. Press)
Ghedini, S., 1982, Software for Photometric Astronomy, (Willmann-Bell Inc.)
Grubbs, F. E. 1950, *Annals of Mathematical Statistics*, **21**, 27 DOI
He, J.-J., Qian, S.-B., 2008, *ChJAA*, **8**, 465 DOI
Henden, A. A., Welch, D. L., Terrell, D., Levine, S. E. 2009, The AAVSO Photometric All-Sky Survey, *AAS*, **214**, 407.02
Henden, A. A., Terrell, D., Welch, D., Smith, T. C. 2010, New Results from the AAVSO Photometric All Sky Survey, *AAS*, **215**, 470.11
Hilditch R. W., King D. J., McFarlane T. M., 1988, *MNRAS*, **231**, 341 DOI
Irwin, J. B., 1952, *ApJ*, **116**, 211 DOI
Irwin, J. B., 1959, *AJ*, **64**, 149 DOI
Kallrath, J. & Milone, E.F., 1998, *Eclipsing Binary Stars–Modeling and Analysis* (Springer-Verlag) DOI
Kopal, Z., 1955, *AnAp*, **18**, 379
Kurucz, R. L., 1979, *ApJS*, **40**, 1 DOI
Kwee, K. K., van Woerden, H., 1956, *BAN*, **12**, 327
McLean, B. J., Hilditch, R. W., 1983, *MNRAS*, **203**, 1 DOI
Mochnacki, S. W., 1981, *ApJ*, **245**, 650 DOI
Nelson, R. H., 2010, "Spectroscopy for Eclipsing Binary Analysis" in The Alt-Az Initiative, Telescope Mirror & Instrument Developments (Collins Foundation Press, Santa Margarita, CA), R.M. Genet, J.M. Johnson and V. Wallen (eds)
Nelson, R. H., 2013, Software by Bob Nelson, `https://www.variablestarssouth.org/bob-nelson/`

[2]O–C Gateway, Paschke, A. `http://var2.astro.cz/ocgate/`

Nelson, R. H., 2014, Spreadsheets, by Bob Nelson,
`https://www.variablestarssouth.org/bob-nelson/`
Nelson, R. H., Şenavci, H. V., Baştürk, Ö, Bahar, E., 2014, *NewA*, **29**, 57 DOI
Nelson, R. H., Terrell, D., Milone, E. F., 2016, *NewAR*, **70**, 1 DOI
Nelson, R. H., 2016, Bob Nelson's O–C Files,
`http://www.aavso.org/bob-nelsons-o-c-files`
Pecaut, M. J., Mamajek, E. E. 2013, *ApJS*, **208**, 9 DOI
Perryman, M. A. C. et al. 1997, *A&A*, **500**, 501,
Qian, S.-B., 2001, *MNRAS*, **328**, 635 DOI
Qian, S.-B., He, J.-J., 2005, *PASJ*, **57**, 977 DOI
Rovithis, P., Rovithis-Livaniou, E., 1984, *A&AS*, **58**, 679
Rovithis-Livaniou, E., Rovithis, P., Djurašević, G., 2002, *IBVS*, **5235**, 1
Rucinski, S. M., 1974, *AcA*, **24**, 119
Rucinski, S M., 2004, *IAUS*, **215**, 17
Russell, H. N., Merrill, J. E., 1952, "The Determination of the Elements of Eclipsing Binary Stars", *Contributions from the Princeton University Observatory*, **26**, 1
Schlegel, D. J., Finkbeiner, D. P., Davis, M., 1998, *ApJ*, **500**, 525 DOI
Smith, T. C., Henden, A., Terrell, D., 2010, AAVSO Photometric All-Sky Survey Implementation at the Dark Ridge Observatory, SAS.
Struve, O., Gratton, L., 1948, *ApJ*, **108**, 497 DOI
Terrell, D., Gross, J., Cooney, W. P. Jr., 2012, *AJ*, **143**, 99 DOI
Terrell, D., 1994, *Van Hamme Limb Darkening Tables, vers. 1.1.*
Van Hamme, W., 1993, *AJ*, **106**, 2096 DOI
Wilson, R. E., Devinney, E. J., 1971, *ApJ*, **166**, 605 DOI
Wilson, R. E., Devinney, E. J., 1973, *ApJ*, **182**, 539 DOI
Wilson, R. E., DeLuccia, M. R., Johnston, K., Mango, S. A., 1972, *ApJ*, **177**, 191 DOI
Wilson, R. E., 1990, *ApJ*, **356**, 613 DOI
Wilson, R. E., 1998, Documentation of Eclipsing Binary Computer Model (available from the author)
Wood F. B., Oliver J. P., Florkowski D. R., Ko h R. H., 1980, *A Finding List for Observers of Interacting Binary Stars*, Univ. of Pennsylvania Press
Wright, C. O., et al., 2003, *AJ*, **125**, 359 DOI
Xiang, F. Y. and Zhou, Y. C., 2004, *NewA*, **9**, 273 DOI
Yildiz, M., Doğan, T., 2013, *MNRAS*, **430**, 2029 DOI
Yildiz, M., 2014, *MNRAS*, **437**, 185 DOI